SIAM J. NUMER. ANAL.
Vol. 50, No. 6, pp. 3110–3133

ANALYSIS OF OPTIMAL SUPERCONVERGENCE OF DISCONTINUOUS GALERKIN METHOD FOR LINEAR HYPERBOLIC EQUATIONS*

YANG YANG† AND CHI-WANG SHU†

Abstract. In this paper, we study the superconvergence of the error for the discontinuous Galerkin (DG) finite element method for linear conservation laws when upwind fluxes are used. We prove that if we apply piecewise kth degree polynomials, the error between the DG solution and the exact solution is $(k+2)$th order superconvergent at the downwind-biased Radau points with suitable initial discretization. Moreover, we also prove the DG solution is $(k+2)$th order superconvergent both for the cell averages and for the error to a particular projection of the exact solution. The superconvergence result in this paper leads to a new a posteriori error estimate. Our analysis is valid for arbitrary regular meshes and for $\mathcal{P}^k$ polynomials with arbitrary $k \geq 1$, and for both periodic boundary conditions and for initial-boundary value problems. We perform numerical experiments to demonstrate that the superconvergence rate proved in this paper is optimal.

Key words. discontinuous Galerkin method, conservation laws, superconvergence, cell average, initial discretization, error estimates, Radau points

AMS subject classifications. 65M60, 65M15

DOI. 10.1137/110857647

1. Introduction.

In this paper, we apply the discontinuous Galerkin (DG) method to one-dimensional linear hyperbolic conservation laws

$$\begin{aligned} &u_t + u_x = 0, && (x,t) \in [0, 2\pi] \times (0, T], \\ &u(x,0) = u_0(x), && x \in R, \end{aligned} \tag{1.1}$$

where the initial datum u_0 is sufficiently smooth. We will consider both the periodic boundary condition $u(0,t) = u(2\pi,t)$ and the initial-boundary value problem with $u(0,t) = g(t)$. We use piecewise kth degree polynomials to approximate the solution in each cell and prove that, under suitable initial discretization, the rate of convergence for the error between the DG solution and the exact solution is of $(k+2)$th order at the downwind-biased Radau points. Moreover, we also prove the $(k+2)$th order superconvergence of the cell averages as well as the error between the DG solution and a particular type of projection of the exact solution.

The DG method was first introduced in 1973 by Reed and Hill [17], in the framework of neutron linear transport. Later, Johnson and Pitkäranta applied the DG method to a scalar linear hyperbolic equation and proved L^p-norm error estimate in [15]. Subsequently, Cockburn et al. developed Runge–Kutta discontinuous Galerkin (RKDG) methods for hyperbolic conservation laws in a series of papers [12, 10, 9, 13]. In [18], Zhang and Shu explicitly gave the formulae of the DG solution in the case of piecewise linear functions for the linear convection equation on uniform meshes. The leading error term is shown to be of a constant magnitude independent of time t. This motivates the division of the numerical error into two parts, one being the leading term and the other being a superconvergent term.

*Received by the editors December 2, 2011; accepted for publication (in revised form) August 6, 2012; published electronically November 29, 2012. This research was supported by DOE grant DE-FG02-08ER25863 and NSF grant DMS-1112700.
http://www.siam.org/journals/sinum/50-6/85764.html
†Division of Applied Mathematics, Brown University, Providence, RI 02912 (yang_yang@brown.edu, shu@dam.brown.edu).

In [2, 3], Adjerid et al. proved the $(k+2)$th order superconvergence of the DG solutions at the downwind-biased Radau points for ordinary differential equations. Later, Adjerid and Weihart [4, 5] investigated the local DG error for multidimensional first order linear symmetric and symmetrizable hyperbolic systems of partial differential equations. The authors showed that the projection of the local DG error is also $(k+2)$th order superconvergent at the downwind-biased Radau points by performing a local error analysis on Cartesian meshes. The global superconvergence is given by numerical experiments. In [4, 5], only initial-boundary value problems are considered, and the local DG error estimate is valid for t sufficiently large. Subsequently, Adjerid and Baccouch [1] investigated the global convergence of the implicit residual-based a posteriori error estimates, and proved that these estimates at a fixed time t converge to the true spatial error in the L^2 norm under mesh refinement. In [7], Cheng and Shu proved $(k+\frac{3}{2})$th order superconvergence of the DG solution towards a particular projection of the exact solution. The authors considered the case of piecewise linear polynomials ($k = 1$) on uniform meshes with periodic boundary conditions for the linear conservation laws. Later Cheng and Shu [8] also proved the same $(k+\frac{3}{2})$th order superconvergence when using piecewise kth degree polynomials with arbitrary k on arbitrary regular meshes. Cheng and Shu also considered both periodic boundary conditions and initial-boundary value problems. However, the convergence rate obtained in [8] is not optimal. Numerical tests showed that the error of the DG solution towards this particular projection of the exact solution is $(k+2)$th order accurate, even on highly nonuniform meshes, when using a special initial discretization. Recently, in [20] Zhong and Shu revisited the same problem and showed that the error between the DG numerical solution and the exact solution is $(k+2)$th order superconvergent at the downwind-biased Radau points and $(2k+1)$th order superconvergent at the downwind point in each cell on uniform meshes with periodic boundary conditions for $k = 1$, 2, and 3. The proofs in [7, 20] use Fourier analysis and work only for uniform meshes and periodic boundary conditions. Moreover, such Fourier analysis is difficult to perform for higher polynomial degree k since it relies explicitly on the structures of algorithm matrices. In [8], a different framework for proving the superconvergence results that does not rely on Fourier analysis is provided and the result is valid for both periodic boundary conditions and initial-boundary value problems. In this paper, we improve upon the result in [8]. A new technique is adopted to obtain the optimal rate of superconvergence. The proof works for arbitrary regular meshes and schemes of any order. Even though the proof in this paper is given for the simple scalar equation (1.1), the same superconvergent results can be easily obtained for one-dimensional linear systems along the same lines.

The organization of this paper is as follows. In section 2, we introduce the DG method under consideration and state the main result. In section 3, we present some preliminaries, including the norms we use throughout the paper, some essential properties of the finite element spaces, DG spatial discretization, as well as the error equations. Section 4 is the main body of the paper where the initial discretization is provided and the main result is proved. Moreover, we also study the application of the superconvergence result in this section. Numerical evidences about the optimality of the superconvergence estimates are given in section 5. We will end in section 6 with some concluding remarks and remarks on future work.

2. DG scheme and statement of the main result. In this section we consider the linear conservation law (1.1). Denote $\Omega = [0, 2\pi]$ to be the computational

domain. First, we divide Ω into N cells

$$0 = x_{\frac{1}{2}} < x_{\frac{3}{2}} < \cdots < x_{N+\frac{1}{2}} = 2\pi,$$

and denote

$$I_j = \left(x_{j-\frac{1}{2}}, x_{j+\frac{1}{2}}\right), \qquad x_j = \frac{1}{2}\left(x_{j-\frac{1}{2}} + x_{j+\frac{1}{2}}\right),$$

as the cells and cell centers, respectively. $h_j = x_{j+\frac{1}{2}} - x_{j-\frac{1}{2}}$ denotes the length of each cell. We also define $h = h_{\max} = \max_j h_j$ and $h_{\min} = \min_j h_j$ to be the lengths of the largest and smallest cells, respectively. In this paper, we consider regular meshes, that is, $h_{\max} \le \lambda h_{\min}$, where $\lambda \ge 1$ is a constant during mesh refinement. Clearly, if $\lambda = 1$, then the mesh is uniformly distributed.

Define

$$V_h = \{v : v|_{I_j} \in \mathcal{P}^k(I_j), j = 1, \ldots, N\}$$

to be the finite element space, where $\mathcal{P}^k(I_j)$ denotes the space of polynomials in I_j of degree at most k. Moreover, we define

$$H_h^1 = \{\phi : \phi|_{I_j} \in H^1(I_j)\ \forall j\}.$$

By using an upwind flux, the DG scheme becomes the following: find $u_h \in V_h$ such that for any $v_h \in V_h$

$$((u_h)_t, v_h)_j = (u_h, (v_h)_x)_j - u_h^- v_h^-|_{j+\frac{1}{2}} + u_h^- v_h^+|_{j-\frac{1}{2}}, \tag{2.1}$$

where $(w, v)_j = \int_{I_j} wv dx$, and $v_h^-|_{j+\frac{1}{2}} = v_h(x_{j+\frac{1}{2}}^-)$ denotes the left limit of the function v_h at $x_{j+\frac{1}{2}}$. Likewise for v_h^+. We also denote $[v_h]_{j+\frac{1}{2}} = v_h(x_{j+\frac{1}{2}}^+) - v_h(x_{j+\frac{1}{2}}^-)$ to be the jump of v_h across $x_{j+\frac{1}{2}}$. For simplicity, we define $\mathcal{H}_j(u_h, v_h)$ to be the right-hand side of (2.1). Then the DG scheme can be written as $((u_h)_t, v_h)_j = \mathcal{H}_j(u_h, v_h)$. Clearly, for any $p(x), q(x) \in H_h^1$,

$$\mathcal{H}_j(p, q) = (p, q_x)_j - p^- q^-|_{j+\frac{1}{2}} + p^- q^+|_{j-\frac{1}{2}} \tag{2.2}$$

$$= -(p_x, q)_j - [p]q^+|_{j-\frac{1}{2}}. \tag{2.3}$$

In addition, if $k \ge 1$, we can define $\mathbb{P}_- u$ to be a Gauss–Radau projection of u into V_h such that

$$(\mathbb{P}_-(u), v)_j = (u, v)_j \quad \forall v \in \mathcal{P}^{k-1}(I_j) \quad \text{and} \quad \mathbb{P}_-(u)(x_{j+1/2}^-) = u(x_{j+1/2}^-). \tag{2.4}$$

Notice that this special projection is used in the error estimates of the DG methods to derive optimal L^2 error bounds in the literature, e.g., in [19]. Like in [8], we will prove that indeed the numerical solution is closer to this special projection of the exact solution than to the exact solution itself.

For the initial discretization, we would like to require

$$u_{ht} = \mathbb{P}_-(u_t) \quad \text{and} \quad \|\mathbb{P}_- u - u_h\|_\Omega = \mathcal{O}(h^{k+2}). \tag{2.5}$$

The exact way to discretize the initial data to achieve the property (2.5) will be given in section 4.1. We can now state our main theorem.

THEOREM 2.1. *Let $u(x,t) \in C^{k+4}$ be the exact solution of the linear hyperbolic equation* (1.1) *and let u_h be the numerical solution of the DG scheme* (2.1). *The finite element space V_h is made up of piecewise polynomials of degree $k \geq 1$ on regular meshes, i.e., the ratio of the length of the largest cell to that of the smallest is bounded during mesh refinement. Then at the time $t = T$ there holds the estimate*

$$\left(\frac{1}{N}\sum_{j=1}^{N}|(u-u_h)(x_j)|^2\right)^{\frac{1}{2}} \leq C(1+T^2)h^{k+2}\|u\|_{k+4,\infty,\Omega}, \tag{2.6}$$

where Ω is the computational domain, and x_j is any one of the downwind-biased Radau points in the cell I_j. The constant C does not depend on h, T, or u.

Remark. Theorem 2.1 is valid for both periodic boundary condition and initial-boundary value problems.

COROLLARY 2.1. *Suppose the conditions in the above theorem are satisfied. Then we have*

$$\|\overline{u-u_h}\|_{L^2(\Omega)} \leq C(1+T^2)h^{k+2}\|u\|_{k+4,\Omega}, \tag{2.7}$$

$$\|\mathbb{P}_- u - u_h\|_{L^2(\Omega)} \leq C(1+T^2)h^{k+2}\|u\|_{k+4,\Omega}, \tag{2.8}$$

where $\overline{u-u_h}$ denotes the cell average of $u-u_h$, and the constant C does not depend on h, T, or u.

3. Preliminaries.

3.1. Norms. We begin by presenting some norms that will be used throughout the paper.

Denote $\|u\|_{0,I_j}$ to be the standard L^2-norm of u on I_j. For any natural number ℓ, we consider the norm and seminorm of the Sobolev space $H^\ell(I_j)$, defined by

$$\|u\|_{\ell,I_j} = \left\{\sum_{0\leq\alpha\leq\ell}\|D^\alpha u\|_{0,I_j}^2\right\}^{1/2}, \quad |u|_{\ell,I_j} = \left\{\sum_{\alpha=\ell}\|D^\alpha u\|_{0,I_j}^2\right\}^{1/2}.$$

For convenience, we use $\|u\|_{I_j}$ to denote $\|u\|_{0,I_j}$.

We also define the L^∞-norm and seminorm by

$$\|u\|_{\ell,\infty,I_j} = \max_{0\leq k\leq\ell}\|D^k u\|_{\infty,I_j}, \quad |u|_{\ell,\infty,I_j} = \|D^\ell u\|_{\infty,I_j},$$

where $\|u\|_{\infty,I_j}$ is the standard L^∞-norm of u on I_j. Clearly, the L^∞-norm is stronger than the L^2-norm, and we have

$$\|u\|_{I_j} \leq h_j^{1/2}\|u\|_{\infty,I_j}. \tag{3.1}$$

Moreover, we define the norms on the whole computational domain as follows:

$$\|u\|_{\ell,\Omega} = \left(\sum_{j=1}^{N}\|u\|_{\ell,I_j}^2\right)^{\frac{1}{2}}, \qquad \|u\|_{\ell,\infty,\Omega} = \max_{1\leq j\leq N}\|u\|_{\ell,\infty,I_j}.$$

3.2. Properties of the finite element space. In this subsection, we study the basic properties of the finite element space. Let us start with the classical inverse properties.

LEMMA 3.1. *Assuming $u \in V_h$, there then exists a constant $C > 0$ independent of h and u such that*

$$\|\partial_x^\alpha u\|_{I_j} \le C h_j^{-\alpha} \|u\|_{I_j}, \qquad \alpha \ge 1, \tag{3.2}$$

$$\left|u^-_{j+\frac{1}{2}}\right| + \left|u^+_{j-\frac{1}{2}}\right| \le C h_j^{-1/2} \|u\|_{I_j}. \tag{3.3}$$

In addition to the projection $\mathbb{P}_-$ defined in (2.4), we also introduce the similar Gauss–Radau projection $\mathbb{P}_+$ of u given on I_j by

$$(\mathbb{P}_+(u), v)_j = (u, v)_j \quad \forall v \in \mathcal{P}^{k-1}(I_j) \quad \text{and} \quad \mathbb{P}_+(u)(x^+_{j-1/2}) = u(x^+_{j-1/2}), \tag{3.4}$$

as well as the standard L^2 projection $\mathbb{P}_k$ by

$$(\mathbb{P}_k(u), v)_j = (u, v)_j \quad \forall v \in \mathcal{P}^k(I_j). \tag{3.5}$$

The projections $\mathbb{P}_+$ and $\mathbb{P}_-$ are distinguished from the exact collocation at different end points of each cell.

Suppose $\mathbb{P}_h$ is a projection, either $\mathbb{P}_k$, $\mathbb{P}_+$, or $\mathbb{P}_-$. Denote the error operator by $\mathbb{P}_h^\perp = \mathbb{I} - \mathbb{P}_h$, where $\mathbb{I}$ is the identity operator. By the scaling argument, we obtain the following lemma [6].

LEMMA 3.2. *Suppose the function $u(x) \in C^{k+1}(I_j)$. Then there exists a positive constant C independent of h and u such that*

$$\|\mathbb{P}_h^\perp u\|_{I_j} \le C h_j^{k+1} |u|_{k+1,I_j} \quad \textit{and} \quad \|\mathbb{P}_h^\perp u\|_{\infty,I_j} \le C h_j^{k+1} |u|_{\infty,k+1,I_j}. \tag{3.6}$$

Moreover, one can also prove the following superconvergence property [2].

LEMMA 3.3. *Suppose $u(x) \in C^{k+2}(I_j)$, and x_j is one of the downwind-biased Radau points in the cell I_j. Then*

$$|(u - \mathbb{P}_- u)(x_j)| \le C h_j^{k+2} |u|_{k+2,\infty,I_j}. \tag{3.7}$$

However, if u is highly oscillatory or discontinuous, we can hardly obtain any useful estimate of $\|\mathbb{P}_h^\perp u\|$ by using the two lemmas above. Therefore, we consider the following estimate.

LEMMA 3.4. *Suppose $u(x)$ is a bounded function. Then*

$$\|\mathbb{P}_h u\|_{\infty,I_j} \le C \|u\|_{\infty,I_j} \quad \textit{and} \quad \|\mathbb{P}_h^\perp u\|_{\infty,I_j} \le C \|u\|_{\infty,I_j}. \tag{3.8}$$

Proof. For the simplicity of presentation, we will prove only for the $\mathbb{P}_-$ projection. We consider the projection on the reference cell $T = [-1, 1]$ and define a special norm in $\mathcal{P}^k(T)$ as

$$|||v||| = \max\left\{ |v(1)|, \left| \int_{-1}^{1} v(s) s^p ds \right| : 0 \le p \le k-1 \right\}.$$

It is not difficult to show this is indeed a norm. Since all norms in $\mathcal{P}^k$ are equivalent, we have $\|v\|_{\infty,T} \le C|||v|||$ for any $v \in \mathcal{P}^k(T)$. Therefore, for any bounded function u,

$$\|\mathbb{P}_- u\|_{\infty,T} \le C|||\mathbb{P}_- u||| = C|||u||| \le C\|u\|_{\infty,T}.$$

This proves the assertion on the reference cell. The general case follows from a standard scaling argument.

By using (3.1) and Lemma 3.4, we obtain

$$\|\mathbb{P}_h^{\perp}u\|_{I_j} \le h_j^{1/2}\|\mathbb{P}_h^{\perp}u\|_{\infty,I_j} \le Ch_j^{1/2}\|u\|_{\infty,I_j}.$$

Now, we move on to the projection of functions depending not only on the spatial variable x but also on the time variable t. Suppose $u(x,t)$ is a function differentiable and integrable with respect to t, and t_1 and t_2 are two real values such that $t_1 < t_2$. Then we have

$$\mathbb{P}_h\left(u_t(x,t)\right) = \left(\mathbb{P}_h u(x,t)\right)_t \quad \text{and} \quad \mathbb{P}_h\left(\int_{t_1}^{t_2} u(x,t)dt\right) = \int_{t_1}^{t_2}(\mathbb{P}_h u(x,t))dt. \tag{3.9}$$

3.3. Properties of the DG spatial discretization. In this subsection, we present some basic properties about the bilinear form $\mathcal{H}_j$. The definitions of $\mathcal{H}_j$ and the two Gauss–Radau projections lead to the following lemma.

LEMMA 3.5. *Suppose $v_h \in V_h$ and $q(x) \in H_h^1$. The two Gauss–Radau projections satisfy the following properties:*

$$\mathcal{H}_j(\mathbb{P}_-^{\perp}q(x), v_h) = 0 \quad \textit{and} \quad \mathcal{H}_j(v_h, \mathbb{P}_+^{\perp}q(x)) = 0. \tag{3.10}$$

Moreover, we define $(u_h, v_h) = \sum_j (u_h, v_h)_j$ and $\mathcal{H}(p,q) = \sum_j \mathcal{H}_j(p,q)$ to obtain the following corollary directly.

COROLLARY 3.1. *Suppose $q(x) \in H_h^1$ and $v_h \in V_h$. There holds*

$$\mathcal{H}(\mathbb{P}_-^{\perp}q(x), v_h) = 0 \quad \textit{and} \quad \mathcal{H}(v_h, \mathbb{P}_+^{\perp}q(x)) = 0. \tag{3.11}$$

3.4. The error equation. In this subsection, we proceed to construct the error equations. Denote the error between the exact solution and the DG numerical solution to be $e(t) = u(t) - u_h(t)$. As the usual treatment in finite element analysis, we divide the considered error into the form $e(t) = \eta(t) - \xi(t)$, where

$$\eta(t) = u(t) - \mathbb{P}_- u(t) \quad \text{and} \quad \xi(t) = u_h(t) - \mathbb{P}_- u(t).$$

From Lemma 3.5, we obtain the error equations of the DG scheme. Suppose $v_h \in V_h$. Then

$$\begin{aligned}(e_t, v_h)_j &= \mathcal{H}_j(e, v_h)\\ &= -\mathcal{H}_j(\xi, v_h)\\ &= -(\xi, v_{hx})_j + \xi^- v_h^-|_{j+\frac{1}{2}} - \xi^- v_h^+|_{j-\frac{1}{2}} \qquad (3.12)\\ &= (\xi_x, v_h)_j + [\xi]v_h^+|_{j-\frac{1}{2}}. \qquad (3.13)\end{aligned}$$

Equations (3.12) and (3.13) are fundamental in our analysis later.

Let us finish this section by proving the following lemma.

LEMMA 3.6. *Suppose $\bar{\xi}$ is the cell average of ξ, that is, $\bar{\xi} = \bar{\xi}_j = \frac{1}{h_j}\int_{I_j}\xi dx$ in cell I_j, for any $j = 1, \ldots, N$. Then we have*

$$\|\xi - \bar{\xi}\|_{I_j} \le Ch_j\|\xi_x\|_{I_j} \le Ch_j\|\mathbb{P}_k e_t\|_{I_j} \le Ch_j\|e_t\|_{I_j}. \tag{3.14}$$

Proof. The right inequality is trivial and the left one follows from the Poincaré inequality. So we need only prove the middle one.

Suppose Q is the Legendre polynomial of degree k in [-1,1], and define $P = (-1)^k Q$. Then P satisfies the following three properties:

(1) P is uniformly bounded: $\|P\|_{\infty,[-1,1]} \leq 1$.

(2) P evaluated at the left boundary is 1: $P(-1) = 1$.

(3) P is orthogonal to any polynomials with degree no greater than $k-1$: $\int_{-1}^{1} PR dx = 0$ for any $R(x) \in \mathcal{P}^{k-1}([-1,1])$.

Define $P_j(x) = P(\frac{2(x-x_j)}{h_j})$. Then P_j also satisfies the corresponding three properties in the cell I_j. In (3.13), we take $v_h = \xi_x - aP_j$, where $a = \xi_x^+|_{j-1/2}$ is a real number, to obtain

$$\begin{aligned} \|\xi_x\|_{I_j}^2 &= (\mathbb{P}_k e_t, \xi_x - aP_j)_j \\ &\leq \|\mathbb{P}_k e_t\|_{I_j} \left(\|\xi_x\|_{I_j} + |a| \|P_j\|_{I_j} \right) \\ &\leq \|\mathbb{P}_k e_t\|_{I_j} \left(\|\xi_x\|_{I_j} + C h_j^{-1/2} \|\xi_x\|_{I_j} h_j^{1/2} \right) \\ &\leq C \|\mathbb{P}_k e_t\|_{I_j} \|\xi_x\|_{I_j}, \end{aligned} \tag{3.15}$$

where the constant C does not depend on j, h or u. Here, for the second step we use the Cauchy–Schwarz inequality, for the third one we use (3.1) and (3.3), and the last step is trivial. We finish the proof by dividing both sides of the above equation by $\|\xi_x\|_{I_j}$.

4. Proof of the main result. This section is the main part of this paper. We first discuss how to discretize the initial datum, then prove the main result, Theorem 2.1, and finally briefly discuss the application of the superconvergence results. The proof can be divided into several steps. Briefly speaking, by using the triangle inequality, we separate $|(u-u_h)(x_j)|$ into two parts, $|(u-\mathbb{P}_- u)(x_j)|$ and $|\xi(x_j)|$. The superconvergence of the first term is given by Lemma 3.3 while the second one is more difficult to deal with and we separate this process into two steps. In the first step, we consider the estimate of e_t as well as e_{tt}. In the second step, we use the quadrature formula and consider the dual problem of (1.1). Besides the main theorem, we also prove Corollary 2.1 in this section.

4.1. The initial discretization. In this subsection we consider the suitable discretization of the initial datum. As mentioned in section 2, we would like to have the initial solution satisfy $\xi_t = 0$ and $\|\xi\|_\Omega \leq Ch^{k+2}$; see (2.5). We start from the requirement $\xi_t = 0$ and check whether a special numerical initial solution can be constructed which also satisfies the second requirement $\|\xi\|_\Omega \leq Ch^{k+2}$. Taking $v_h = 1$ in (3.12), we have the following lemma

LEMMA 4.1. *$\int_{I_j} e_t dx = 0 \ \forall\ 1 \leq j \leq N$ if and only if $\xi_{j+\frac{1}{2}}^-$ is a constant which does not depend on j.*

Denote the constant mentioned in the previous lemma as S. Clearly, such a constant gives us freedom to control $\|\xi\|_{I_j}$, and this is shown in the following lemma.

LEMMA 4.2. *Suppose $\|e_t\|_{I_j} \leq Ch_j^{k+3/2}$. Then $S \leq Ch_j^{k+2}$ if and only if $\|\xi\|_{I_j} \leq Ch_j^{k+5/2}$.*

Proof. Suppose $\|\xi\|_{I_j} \le Ch_j^{k+5/2}$. Then by Lemma 3.1 we have $S \le Ch_j^{k+2}$. On theother hand, suppose $S \le Ch_j^{k+2}$. Then by Lemma 3.6

$$\begin{aligned}\bar{\xi}_j &= \xi^-_{j+\frac{1}{2}} - (\xi - \bar{\xi}_j)^-_{j+\frac{1}{2}} \\ &\le S + Ch_j^{-1/2}\|\xi - \bar{\xi}_j\|_{I_j} \\ &\le S + Ch_j^{1/2}\|e_t\|_{I_j} \\ &\le Ch_j^{k+2}.\end{aligned}$$

Therefore,

$$\|\xi\|_{I_j} \le \|\bar{\xi}_j\|_{I_j} + \|\xi - \bar{\xi}_j\|_{I_j} \le Ch_j^{k+5/2}.$$

Remark. The condition $\|e_t\|_{I_j} \le Ch_j^{k+3/2}$ in Lemma 4.2 is true because we require $\xi_t = 0$. Actually, we can show $\|e_t\|_{I_j} \le Ch_j^{k+1}|u|_{k+2,I_j}$. We will also use this estimate of e_t later in this subsection.

There is a straightforward corollary of the above lemma.

COROLLARY 4.1. *Suppose the initial solution satisfies $\xi_t = 0$ and $S \le Ch^{k+2}$. Then $\|\xi\|_\Omega \le Ch^{k+2}$.*

Now let us proceed to construct the initial solution u_h from $\xi_t = 0$.

LEMMA 4.3. *Suppose $\int_{I_j} e_t = 0$. Then ξ_x is uniquely determined by $\mathbb{P}_k e_t$ in the cell I_j.*

Proof. Let $v_h^+|_{j-\frac{1}{2}} = 0$ in (3.13). Then we have

$$(\mathbb{P}_k e_t, v_h)_j = (\xi_x, v_h)_j. \tag{4.1}$$

Since the equation above is linear, we need only prove the uniqueness. That is, suppose $(\mathbb{P}_k e_t, v_h)_j = 0 \ \forall\ v_h \in V_h$ and $v_h^+|_{j-\frac{1}{2}} = 0$. Then we need to show $\xi_x = 0$. To prove this, let $p(x)$ be an arbitrary polynomial of degree no more than k and $v_h = p - p^+_{j-\frac{1}{2}}$. Then

$$(\mathbb{P}_k e_t, p)_j = (\mathbb{P}_k e_t, p - p^+_{j-\frac{1}{2}})_j = 0.$$

This implies that $\mathbb{P}_k e_t = 0$. By Lemma 3.6, we obtain $\xi_x = 0$.

Remark. The expression of u_t can be obtained by the PDE; therefore, it is not difficult to obtain $\mathbb{P}_k e_t$ from $\xi_t = 0$.

Now, the only thing left is to determine the value of the constant $S = \xi^-_{j-\frac{1}{2}}$. By Corollary 4.1 we can simply take $S = 0$. However, such S does not satisfy the conservation of mass. If we consider periodic boundary condition, then we can select a special S such that $\int_\Omega \xi = 0$. We first prove that such S satisfies the property $S \le Ch^{k+2}$. Actually,

$$\int_\Omega \xi dx = \sum_{j=1}^N \bar{\xi}_j h_j = \sum_{j=1}^N \left(S - (\xi - \bar{\xi})^-_{j+\frac{1}{2}}\right) h_j,$$

which yields

$$S|\Omega| = \sum_{j=1}^N (\xi - \bar{\xi})^-_{j+\frac{1}{2}} h_j. \tag{4.2}$$

Then we obtain

$$S \le \frac{C}{|\Omega|}\sum_{j=1}^{N}\|e_t\|_{I_j}h_j^{3/2} \le \frac{C}{|\Omega|}\left(\sum_{j=1}^{N}h_j^{2k+5}\right)^{1/2}|u|_{k+2,\Omega} \le \frac{C}{\sqrt{|\Omega|}}h^{k+2}|u|_{k+2,\Omega}. \tag{4.3}$$

In the first inequality in (4.3) we use Lemma 3.6 and (3.3). For the second inequality we use Cauchy–Schwarz inequality and the estimate $\|e_t\|_{I_j} \le Ch_j^{k+1}|u|_{k+2,I_j}$, which is obtained in the remark after Lemma 4.2. The last inequality follows from the fact that $\sum h_j = |\Omega|$ and $h_j \le h$.

Now we summarize how to implement the initial discretization. We divide the process into the following steps:

(1) Let $\xi_t = 0$, then compute the value of e_t with the help of the PDE.

(2) Use Lemma 4.3 to find out ξ_x.

(3) Compute $\xi - \bar{\xi}$ in each cell from the expression of ξ_x and the fact that $\int_{I_j}(\xi - \bar{\xi})dx = 0$.

(4) Work out S by using (4.2) or simply by taking $S = 0$.

(5) Calculate ξ from the expressions of S and ξ_x.

(6) Figure out $u_h = \xi + \mathbb{P}_- u$.

From the process mentioned above, we can observe that the initial solution is uniquely determined by the requirements $\xi_t = 0$ and $\int_\Omega \xi dx = 0$ or $\xi^-_{j-\frac{1}{2}} = 0$.

4.2. Step 1. Now, we proceed to prove Theorem 2.1. The estimates of $\|e_t\|_\Omega$ and $\|e_{tt}\|_\Omega$ follow from Lemma 2.3 in [8] with some minor changes, so we skip the proof and only state the results in the following two equations:

$$\|e_{tt}(t)\|_\Omega \le Ch^{k+1}|u|_{k+3,\Omega} + Cth^{k+1}|u|_{k+4,\Omega}, \tag{4.4}$$

$$\|e_t(t)\|_\Omega \le Ch^{k+1}|u|_{k+2,\Omega} + Cth^{k+1}|u|_{k+3,\Omega}. \tag{4.5}$$

Therefore, by Lemma 3.6 we have

$$\|\xi - \bar{\xi}\| \le C(1+t)h^{k+2}\|u\|_{k+3,\Omega}. \tag{4.6}$$

Before proceeding to the optimal error estimates of $\|\xi\|_\Omega$, we use the following superconvergence result to prove the optimal error estimate of $\|e\|_{\infty,\Omega}$ to end this subsection.

Following [8], we can easily prove

$$\|\xi(t)\|_\Omega \le C(1+t)h^{k+3/2}\|u\|_{k+3,\Omega}.$$

Since ξ is a polynomial of degree at most k in each cell, we have

$$\|\xi(t)\|_{\infty,I_j} \le Ch^{-1/2}\|\xi(t)\|_{I_j} \le Ch^{-1/2}\|\xi(t)\|_\Omega \le C(1+t)h^{k+1}\|u\|_{k+3,\Omega}.$$

Notice that the right-hand side of the above equation does not depend on j. We can therefore take the maximum on both sides to obtain

$$\|\xi(t)\|_{\infty,\Omega} \le C(1+t)h^{k+1}\|u\|_{k+3,\Omega}.$$

Finally, by Lemma 3.2, we obtain

$$\|e(t)\|_{\infty,\Omega} \le C(1+t)h^{k+1}\|u\|_{\infty,k+3,\Omega}.$$

4.3. Step 2. Now, we proceed to estimate $e(x_j)$. By Lemma 3.3, only $\xi(x_j)$ is considered. Denote the downwind-biased Radau points of the cell I_j as x_j^i, $0 \le i \le k$. Also denote ψ_j^i to be a polynomial of degree k in cell I_j such that

$$\psi_j^i(x_\ell) = \begin{cases} 1 & x_\ell = x_j^i, \\ 0 & x_\ell \neq x_j^i. \end{cases} \tag{4.7}$$

By the Gauss–Radau quadrature $\xi(x_j^i) = \frac{2}{w_i h_j}(\xi, \psi_j^i)$, where the constant w_i is the weight of the quadrature at the ith downwind-biased Radau point on the reference interval $[-1, 1]$. Based on this quadrature, we need only estimate (ξ, ψ_j^i) for any $0 \le i \le k$. Clearly, $\|\psi_j^i\|_\infty \le C$, where the positive constant C does not depend on i, j, or h. Motivated by [11], we consider the dual problem of (1.1). For convenience, below we denote by C a generic positive constant that does not depend on h, T, or u, but may depend on λ, recalling that λ is the ratio of the length of the largest cell to that of the smallest.

We begin by considering the solution to the dual problem:

(1) For the periodic boundary condition, find a function ϕ_j^i such that $\phi_j^i(\cdot, t)$ satisfies

$$\begin{array}{ll} \phi_{j\,t}^i + \phi_{j\,x}^i = 0, & (x,t) \in R \times (0,T], \\ \phi_j^i(x,T) = \psi_j^i(x), & x \in R, \\ \phi_j^i(0,t) = \phi_j^i(2\pi,t), & t \in [0,T]. \end{array} \tag{4.8}$$

(2) For the initial boundary value problem, find a function ϕ_j^i such that $\phi_j^i(\cdot, t)$ satisfies

$$\begin{array}{ll} \phi_{j\,t}^i + \phi_{j\,x}^i = 0, & (x,t) \in R \times (0,T], \\ \phi_j^i(x,T) = \psi_j^i(x), & x \in R, \\ \phi_j^i(2\pi,t) = 0, & t \in [0,T]. \end{array} \tag{4.9}$$

For convenience, we drop the subscript j as well as the superscript i and denote ψ to be ψ_j^i and ϕ to be ϕ_j^i in this section. Following [11]

$$\begin{aligned} (e(T), \psi) &= (e, \phi)(0) + \int_0^T (e, \phi)_t dt \\ &= (e, \phi)(0) + \int_0^T [(e_t, \phi) + (e, \phi_t)] dt. \end{aligned} \tag{4.10}$$

We apply $\mathbb{P}_+$ to deal with the term $(e_t, \phi) + (e, \phi_t)$, with the definition of the projection given in (3.4). Recalling that $e = \eta - \xi$, where the notations of ξ and η can be found at the beginning of section 3.4, we have

$$\begin{aligned} (e_t, \phi) + (e, \phi_t) &= (e_t, \mathbb{P}_+^\perp \phi) + (e_t, \mathbb{P}_+ \phi) - (e, \phi_x) \\ &= (e_t, \mathbb{P}_+^\perp \phi) + \mathcal{H}(e, \mathbb{P}_+ \phi) - (\eta, \phi_x) + (\xi, \phi_x) \\ &= (e_t, \mathbb{P}_+^\perp \phi) - \mathcal{H}(\xi, \mathbb{P}_+ \phi) - (\eta, \phi_x) + \mathcal{H}(\xi, \phi) \\ &\quad - \sum_{j=2}^{N} \xi^- [\phi]_{j-\frac{1}{2}} + \xi^- \phi^-|_{N+\frac{1}{2}} - \xi^- \phi^+|_{\frac{1}{2}} \\ &= (e_t, \mathbb{P}_+^\perp \phi) - (\eta, \phi_x) - \sum_{j=2}^{N} \xi^- [\phi]_{j-\frac{1}{2}} + \xi^- \phi^-|_{N+\frac{1}{2}} - \xi^- \phi^+|_{\frac{1}{2}}, \end{aligned} \tag{4.11}$$

where for the last equality we use Corollary 3.1.

For the periodic boundary condition, the above turns out to be

$$(e_t,\phi)+(e,\phi_t)=(e_t,\mathbb{P}_+^{\perp}\phi)-(\eta,\phi_x)-\sum_{j=1}^{N}\xi^-[\phi]_{j-\frac{1}{2}}. \tag{4.12}$$

Integrating in t and noticing the fact that

$$\int_0^T\sum_{j=1}^{N}\xi^-[\phi]_{j-\frac{1}{2}}=0$$

since $[\phi(t)]_{i-\frac{1}{2}}=0$ except for at most finitely many t, we have

$$\int_0^T[(e_t,\phi)+(e,\phi_t)]dt=\int_0^T(e_t,\mathbb{P}_+^{\perp}\phi)dt+\int_0^T(\eta,\phi_t)dt. \tag{4.13}$$

For the initial boundary value problem, keeping in mind the fact that $\xi^-_{\frac{1}{2}}=0$, (4.11) becomes

$$(e_t,\phi)+(e,\phi_t)=(e_t,\mathbb{P}_+^{\perp}\phi)-(\eta,\phi_x)-\sum_{j=2}^{N}\xi^-[\phi]_{j-\frac{1}{2}}+\xi^-\phi^-|_{N+\frac{1}{2}}. \tag{4.14}$$

Integrating the above equation in t, and noticing the fact that

$$\int_0^T\sum_{j=1}^{N}\xi^-[\phi]_{j-\frac{1}{2}}=0\quad\text{and}\quad\int_0^T\xi^-\phi^-|_{N+\frac{1}{2}}=0$$

since $[\phi(t)]_{i-\frac{1}{2}}=0$ except for at most finitely many t, and $\phi^-(t)|_{N+\frac{1}{2}}=0$ when $t<T$, we again obtain (4.13).

We use integration by parts on the second term of the right-hand side of (4.13),

$$\int_0^T(\eta,\phi_t)dt=(\eta,\psi)(T)-(\eta,\phi)(0)-\int_0^T(\eta_t,\phi)dt. \tag{4.15}$$

Plugging (4.15) into the second term on the right-hand side of (4.13), then plugging (4.13) into the right-hand side of (4.10), we obtain

$$(e(T),\psi)=(e,\phi(0))+\int_0^T(e_t,\mathbb{P}_+^{\perp}\phi)dt+(\eta,\psi)(T)-(\eta,\phi)(0)-\int_0^T(\eta_t,\phi)dt.$$

Noticing the fact that $\mathbb{P}_-u-u_h=e-\eta$, we have

$$(\mathbb{P}_-u-u_h,\psi)(T)=\Pi_1^j+\Pi_2^j+\Pi_3^j,$$

where

$$\Pi_1^j=(\mathbb{P}_-u-u_h,\phi)(0),$$

$$\Pi_2^j=-\int_0^T(\mathbb{P}_-^{\perp}u_t,\phi)dt,$$

$$\Pi_3^j=\int_0^T(e_t,\mathbb{P}_+^{\perp}\phi)dt.$$

For the first term, notice the fact that at $t = 0$, the support of ϕ_j is of length at least $h_{\min}$. Therefore, each cell contains at most $\lceil\lambda\rceil + 1$ such ϕ_j, where $\lceil\lambda\rceil$ denotes the smallest integer no smaller than λ. In section 4.1 we obtain the estimate $\|\xi(0)\|_\Omega \le Ch^{k+2}|u|_{k+2,\Omega}$. Then

$$\begin{aligned}\sum_{j=1}^{N}(\Pi_1^j)^2 &= \sum_{j=1}^{N}(\mathbb{P}_-u - u_h, \phi_j)^2(0)\\ &\le Ch(\lceil\lambda\rceil+1)\|\xi\|_\Omega^2\\ &\le Ch^{2k+5}|u|_{k+2,\Omega}^2. \end{aligned} \tag{4.16}$$

4.3.1. The estimate of Π_2^j. In this subsubsection, we proceed to estimate $\Pi_2^j = -\int_0^T(\mathbb{P}_-^\perp u_t, \phi)$. For simplicity, only the periodic boundary condition is considered; however, the estimate of the initial-boundary value problem can be obtained in exactly the same way. We extend our meshes onto the whole real line periodically, so the domain under consideration in this and the next subsections is $R \times [0, T]$. Clearly, the characteristic line which passes through $(x_{j-\frac{1}{2}}, T)$, denoted by l_j, is $t = x + T - x_{j-\frac{1}{2}}$, $0 < t < T$. We also assume that l_j and the cell boundary $x_{i-\frac{1}{2}} \times [0, T]$ intersect at $t = t_i^j$. Denote the support of ϕ in $R\times[0, T]$ as Ω_j. Then the boundaries of the cells separate Ω_j into several pieces, as shown in Figure 4.1. Denote $\Omega_i^j = \Omega_j \cap I_i \times [0, T]$ and $k_j = \min\{i : \Omega_i^j \text{ is not empty}\}$. Also define $\Delta_j = \{k_j, k_j + 1, \dots, j\}$ to be the index set which contains the subscripts of all the nonempty pieces. Then we can easily figure out the following properties:

(1) $\Omega_j = \cup_{i\in\Delta_j}\Omega_i^j$ and $|\Delta_j| = j - k_j + 1 \le \lceil\frac{T\lambda}{h}\rceil + 1$.

(2) Denote $\widetilde{\Delta}_j = \{i \in \Delta_j | \Omega_i^j \text{ is not a parallelogram}\}$. Then $|\widetilde{\Delta}_j| \le \lceil\lambda\rceil + 2$ and $j \in \widetilde{\Delta}_j$.

(3) Among those which are not parallelograms, Ω_j^j is a triangle which lies in the region $R \times [T - h, T]$, and by denoting $\widetilde{\Omega}_j = \cup_{i\in\widetilde{\Delta}_j\setminus j}\Omega_i^j$, we have $\widetilde{\Omega}_j \in R \times [0, 2h]$.

(4) Suppose Ω_i^j is a parallelogram. Then the vertices are $(x_{i-\frac{1}{2}}, t_i^j)$, $(x_{i+\frac{1}{2}}, t_{i+1}^j)$, $(x_{i+\frac{1}{2}}, t_{i+1}^{j+1})$, and $(x_{i-\frac{1}{2}}, t_i^{j+1})$.

Now we can proceed to the estimate

$$\int_0^T(\mathbb{P}_-^\perp u_t, \phi) = \sum_{i\in\Delta_j}\int_{\Omega_i^j}\mathbb{P}_-^\perp u_t\ \phi\ dxdt.$$

Consider the parallelogram Ω_i^j. Noticing the fact that

$$\begin{aligned}\int_{t_i^{j+1}}^{t_{i+1}^j}\left(\mathbb{P}_-^\perp u_t(t_i^{j+1}), \phi\right)dt &= \left(\mathbb{P}_-^\perp u_t(t_i^{j+1}), \int_{t_i^{j+1}}^{t_{i+1}^j}\phi\ dt\right)\\ &= \left(\mathbb{P}_-^\perp u_t(t_i^{j+1}), \int_{I_j}\psi\ dx\right)\\ &= 0, \end{aligned} \tag{4.17}$$

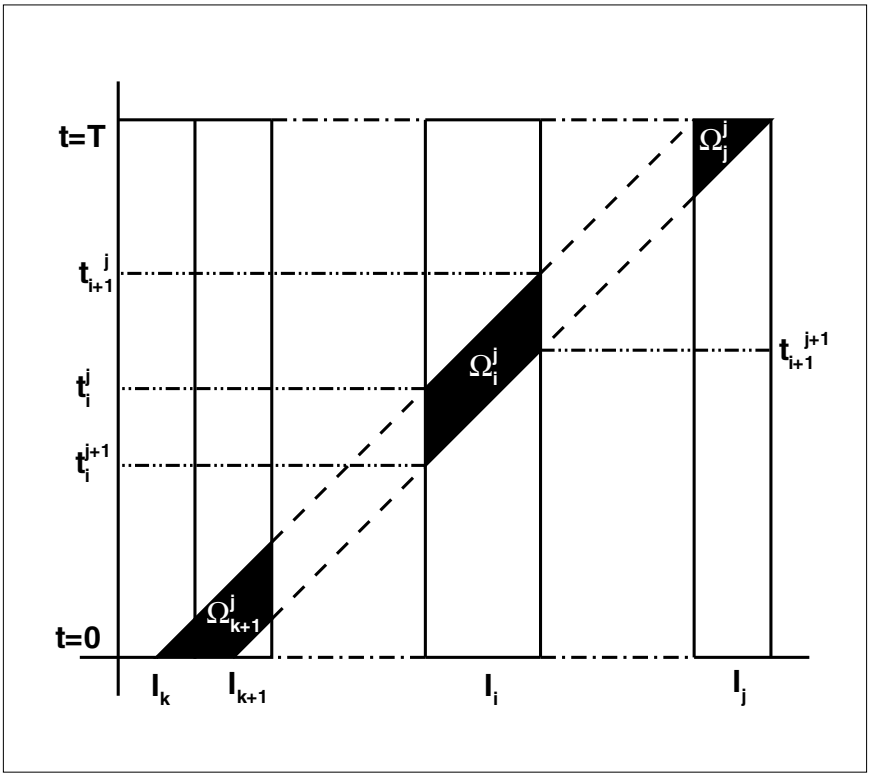

FIG. 4.1. *The support of ϕ: black polygons along the dashed line.*

we then have

$$\begin{aligned}
\int_{\Omega_i^j} \mathbb{P}_-^{\perp} u_t \ \phi \ dxdy &= \int_{t_i^{j+1}}^{t_{i+1}^j} (\mathbb{P}_-^{\perp} u_t, \phi) dt \\
&= \int_{t_i^{j+1}}^{t_{i+1}^j} (\mathbb{P}_-^{\perp} u_t(t) - \mathbb{P}_-^{\perp} u_t(t_i^{j+1}), \phi) dt \\
&= \int_{t_i^{j+1}}^{t_{i+1}^j} \left(\mathbb{P}_-^{\perp} \left(\int_{t_i^{j+1}}^{t} u_{tt}(\tau) d\tau \right), \phi \right) dt \\
&= \int_{t_i^{j+1}}^{t_{i+1}^j} \int_{t_i^{j+1}}^{t} \left(\mathbb{P}_-^{\perp} u_{tt}(\tau), \phi \right) d\tau dt \\
&\leq C h^{k+4} |u|_{k+3,\infty,\Omega}. \qquad (4.18)
\end{aligned}$$

Now, we consider Ω_j^j and $\widetilde{\Omega}_j$. By using the third property of the partition of the support of Ω_j, we have

$$\int_{\Omega_j^j} \mathbb{P}_-^{\perp} u_t \ \phi \ dxdt \leq C h^{k+3} |u|_{k+2,\infty,\Omega}$$

and

$$\int_{\widetilde{\Omega}_j} \mathbb{P}_-^{\perp} u_t \ \phi \ dxdt \le Ch^{k+3}|u|_{k+2,\infty,\Omega}.$$

Combining the above, we obtain

$$\int_0^T (\mathbb{P}_-^{\perp} u_t, \phi) \le Ch^{k+3}|u|_{k+2,\infty,\Omega} + CTh^{k+3}|u|_{k+3,\infty,\Omega}.$$

4.3.2. The estimate of Π_3^j. In this subsubsection, we still consider periodic boundary conditions and follow the procedure in the previous subsubsection. However, there are two differences:

(1) The support of $\mathbb{P}_+^{\perp}\phi$, denoted as T_j, is different from Ω_j.

(2) We do not have the local estimate of $\|e_{tt}\|_{I_j}$ or $\|e_t\|_{I_j}$.

To deal with the first one, we define $T_i^j = T_j \cap I_i \times (0,T)$. Clearly T_i^j is a rectangle covering Ω_i^j and can be written as $T_i^j = I_i \times (t_0, t_1)$, where $t_0 = \inf\{t : \exists x \in I_i$ such that (s.t.) $(x,t) \in \Omega_i^j\}$ and $t_1 = \sup\{t : \exists x \in I_i$ s.t. $(x,t) \in \Omega_i^j\}$. Clearly, if Ω_i^j is a parallelogram, then $t_0 = t_i^{j+1}$ and $t_1 = t_{i+1}^j$ (see Figure 4.2). We also denote $\widetilde{T}_j = \cup_{i \in \widetilde{\Delta}_j \setminus j} T_i^j$. Then $T_j = \cup_{i \in \Delta_j} T_i^j$. Moreover, it is not difficult to obtain

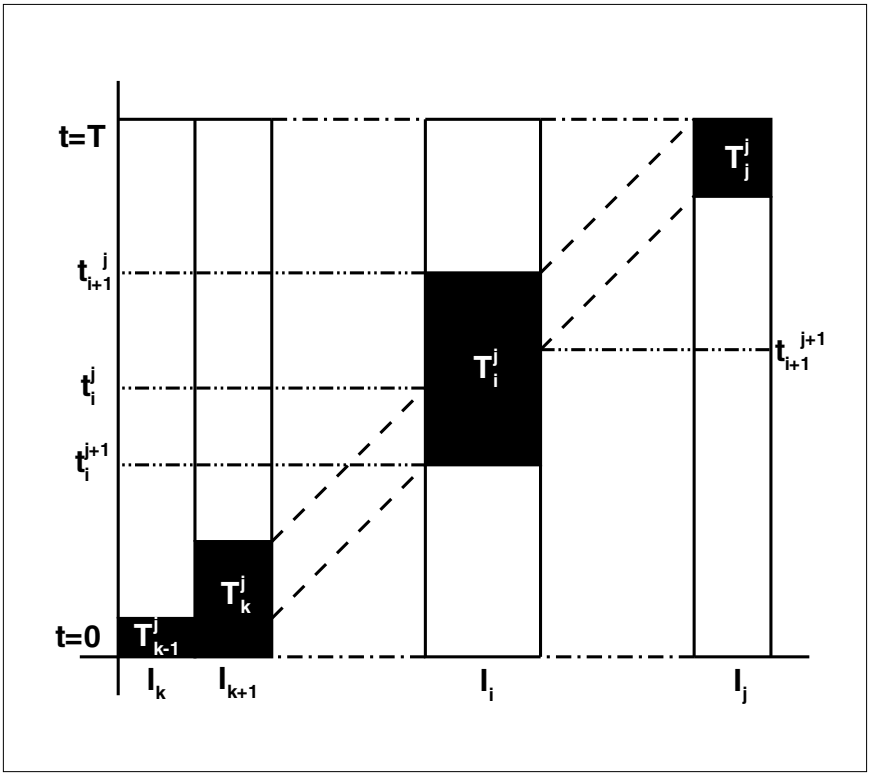

FIG. 4.2. *The support of $\mathbb{P}_+\phi$: the black boxes along the dashed line.*

$T_j^j \subset I_j \times (T-h, T)$ and $\widetilde{T}_j \subset R \times (0, 2h)$. Consider T_i^j such that Ω_i^j is a parallelogram. Notice the fact that

$$\begin{aligned}\int_{t_i^{j+1}}^{t_{i+1}^j} (e_t(t_i^{j+1}), \mathbb{P}_+^{\perp}\phi)dt &= \left(e_t(t_i^{j+1}), \mathbb{P}_+^{\perp}\int_{t_i^{j+1}}^{t_{i+1}^j} \phi \; dt\right) \\ &= \left(e_t(t_i^{j+1}), \mathbb{P}_+^{\perp}\int_{I_j} \psi \; dx\right) \\ &= 0. \end{aligned} \tag{4.19}$$

Then we have

$$\begin{aligned}\int_{T_i^j} e_t \; \mathbb{P}_+^{\perp}\phi \; dxdt &= \int_{t_i^{j+1}}^{t_{i+1}^j} (e_t, \mathbb{P}_+^{\perp}\phi)dt \\ &= \int_{t_i^{j+1}}^{t_{i+1}^j} \left(e_t(t) - e_t(t_i^{j+1}), \mathbb{P}_+^{\perp}\phi\right) dt \\ &= \int_{t_i^{j+1}}^{t_{i+1}^j} \left(\int_{t_i^{j+1}}^{t} e_{tt}(\tau)d\tau, \mathbb{P}_+^{\perp}\phi\right) dt \\ &\le Ch^{3/2} \int_{t_i^{j+1}}^{t_{i+1}^j} \|e_{tt}\|_{I_i} dt. \end{aligned} \tag{4.20}$$

Observe that $\sup\{t : (x,t) \in \widetilde{T}_j\} \le 2h$ and $\inf\{t : (x,t) \in T_j^j\} \ge T-h$; therefore,

$$\int_{T_j^j} e_t \; \mathbb{P}_+^{\perp}\phi \; dxdt \le Ch_j^{1/2} \int_{T-h}^{T} \|e_t\|_{I_j} dt$$

and

$$\begin{aligned}\int_{\widetilde{T}_j} e_t \; \mathbb{P}_+^{\perp}\phi \; dxdt &\le C \int_0^{2h} \sum_{i \in \widetilde{\Delta}_j \setminus j} \|e_t\|_{I_i} h_i^{1/2} dt \\ &\le Ch^{1/2} \int_0^{2h} \left(\sum_{i \in \widetilde{\Delta}_j \setminus j} \|e_t\|_{I_i}^2\right)^{1/2} dt. \end{aligned} \tag{4.21}$$

Combining the above, we obtain the following estimate:

$$\Pi_3^j \le C\Gamma_1^j + C\Gamma_2^j + C\Gamma_3^j,$$

where

$$\Gamma_1^j = h^{3/2} \sum_{i \in \Delta_j \setminus \widetilde{\Delta}_j} \int_{t_i^{j+1}}^{t_{i+1}^j} \|e_{tt}\|_{I_i} dt,$$

$$\Gamma_2^j = h_j^{1/2} \int_{T-h}^{T} \|e_t\|_{I_j} dt,$$

$$\Gamma_3^j = h^{1/2} \int_0^{2h} \left(\sum_{i \in \widetilde{\Delta}_j \setminus j} \|e_t\|_{I_i}^2\right)^{1/2} dt.$$

As mentioned at the beginning of this subsection, we do not have the local estimate of $\|e_t\|$ or $\|e_{tt}\|$, so we need to consider the summation with respect to j.

First, we consider Γ_1^j. Keeping in mind the fact that, for any $t \in (0,T)$ and $1 \le i \le N$, the information of $\|e_{tt}(t)\|_{I_i}$ is contained in at most $\lceil \lambda \rceil + 1$ many of Γ_1^j, we then have

$$\begin{aligned}
\sum_{j=1}^{N} |\Gamma_1^j|^2 &\le \sum_{j=1}^{N} h^3 \sum_{i \in \Delta_j \setminus \widetilde{\Delta}_j} \left\lceil \frac{T\lambda}{h} \right\rceil \left(\int_{t_i^{j+1}}^{t_{i+1}^j} \|e_{tt}\|_{I_i} dt \right)^2 \\
&\le CTh^3 \sum_{j=1}^{N} \sum_{i \in \Delta_j \setminus \widetilde{\Delta}_j} \int_{t_i^{j+1}}^{t_{i+1}^j} \|e_{tt}\|_{I_i}^2 dt \\
&\le CT(\lceil \lambda \rceil + 1) h^3 \int_0^T \|e_{tt}\|_\Omega^2 dt \\
&\le CTh^{2k+5} \int_0^T (|u|_{k+3,\Omega} + t|u|_{k+4,\Omega})^2 dt \\
&\le Ch^{2k+5} \left(T^2 |u|_{k+3,\Omega}^2 + T^4 |u|_{k+4,\Omega}^2 \right). \qquad (4.22)
\end{aligned}$$

The second term is easy to deal with:

$$\begin{aligned}
\sum_{j=1}^{N} |\Gamma_2^j|^2 &\le \sum_{j=1}^{N} h^2 \int_{T-h}^{T} \|e_t\|_{I_j}^2 dt \\
&= h^2 \int_{T-h}^{T} \|e_t\|_\Omega^2 dt \\
&\le Ch^{2k+4} \int_{T-h}^{T} (|u|_{k+2,\Omega} + t|u|_{k+3,\Omega})^2 dt \\
&\le Ch^{2k+5} \left(|u|_{k+2,\Omega}^2 + T^2 |u|_{k+3,\Omega}^2 \right) dt. \qquad (4.23)
\end{aligned}$$

The third term is also not difficult. Noticing the fact that for fixed i, $\int_0^{2h} \|e_t\|_{I_i}$ is contained in at most $\lceil \lambda \rceil + 1$ many of Γ_3^j, we have

$$\begin{aligned}
\sum_{j=1}^{N} |\Gamma_3^j|^2 &\le \sum_{j=1}^{N} h^2 \int_0^{2h} \sum_{i \in \tilde{\Delta}_j \setminus j} \|e_t\|_{I_j}^2 dt \\
&\le (\lceil \lambda \rceil + 1) h^2 \int_0^{2h} \|e_t\|_\Omega^2 dt \\
&\le Ch^{2k+4} \int_0^{2h} (|u|_{k+2,\Omega} + t|u|_{k+3,\Omega})^2 dt \\
&\le Ch^{2k+5} \left(|u|_{k+2,\Omega}^2 + h^2 |u|_{k+3,\Omega}^2 \right) dt. \qquad (4.24)
\end{aligned}$$

Combining the above we obtain

$$\sum_{j=1}^{N} |\Pi_3^j|^2 \le C \sum_{j=1}^{N} \left(|\Gamma_1^j|^2 + |\Gamma_2^j|^2 + |\Gamma_3^j|^2 \right) \le C(1+T^4) h^{2k+5} \|u\|_{k+4,\Omega}^2.$$

Remark. By the same method mentioned in this subsection, we can also derive that

$$\sum_{j=1}^{N} |\Pi_2^j|^2 \le C(1+T^2)h^{2k+5}\|u\|_{k+4,\Omega}^2.$$

Here the upper bound is of T^2 instead of T^4 since $\|\eta_t\|_\Omega$ and $\|\eta_{tt}\|_\Omega$ do not grow in time.

4.4. Final estimate. Now we proceed to the final estimate of $|\xi(x_j)|$. We simply sum up all the previous estimates and obtain

$$\begin{aligned}\sum_{j=1}^{N} |(\xi,\psi_j)|^2 &\le 3\sum_{j=1}^{N}\left(|\Pi_1^j|^2+|\Pi_2^j|^2+|\Pi_3^j|^2\right)\\ &\le Ch^{2k+5}\left(|u|_{k+2,\Omega}^2+(1+T^2)\|u\|_{k+4,\Omega}^2+(1+T^4)\|u\|_{k+4,\Omega}^2\right)\\ &\le Ch^{2k+5}(1+T^4)\|u\|_{k+4,\Omega}^2. \qquad (4.25)\end{aligned}$$

Therefore,

$$\begin{aligned}\frac{1}{N}\sum_{j=1}^{N}|\xi(x_j)|^2 &= \frac{1}{N}\sum_{j=1}^{N}\left|\frac{2}{h_j}(\xi,\psi_j)\right|^2\\ &\le Ch^{2k+4}(1+T^4)\|u\|_{k+4,\Omega}^2.\end{aligned}$$

By Lemma 3.3,

$$\frac{1}{N}\sum_{j=1}^{N}|(u-u_h)(x_j)|^2 \le Ch^{2k+4}(1+T^4)\|u\|_{k+4,\infty,\Omega}^2. \qquad (4.26)$$

We have now finished the proof of the main theorem.

Noticing the fact that, throughout the whole proof, we have not used any special property of ψ, we can then take ψ to be the indicator function of the cell I_j, which yields the estimate of (2.7). Finally, (2.8) follows from (4.6) and (2.7).

4.5. Applications. In section 4.2, we proved the optimal error estimates in the L^∞-norm by using the superconvergence of $\xi = u_h - \mathbb{P}_- u$. This can be considered as an application of the superconvergence result. We also briefly discuss another application in using the superconvergence of the cell averages for a new a posterior error indicator, in the same spirit as in [16] where the jump sizes at cell interfaces are used as an a posterior error indicator. For simplicity of notation, we denote v as the numerical solution instead of u_h in this section and consider the cell I_j only. Due to the superconvergence result, the cell average of the numerical solution $\overline{v_j}$ is superclose to that of the exact solution $\overline{u_j}$. If we construct another numerical cell average $\widetilde{v_j}$ which is not superconvergent, then the difference $\widetilde{v_j} - \overline{v_j}$ is a good a posterior error indicator of the local error. We construct $\widetilde{v_j}$ in the following steps:

(1) Extend the polynomial numerical solution from the two neighboring cells, denoted by v_{j-1} and v_{j+1}, to the cell I_j.

(2) Compute the cell averages of v_{j-1} and v_{j+1} in the cell I_j, and denote them by $\widetilde{v_{j-1}}$ and $\widetilde{v_{j+1}}$, respectively.

(3) Define

$$\widetilde{v_j} = \theta\widetilde{v_{j-1}} + (1-\theta)\widetilde{v_{j+1}},$$

where $0 \le \theta \le 1$. In general, the new cell average $\widetilde{v_j}$ is only $(k+1)$th order accurate.

(4) The a posterior computable quantity $\widetilde{v_j} - \overline{v_j}$ is asymptotically equal to the error $\widetilde{v_j} - \overline{u_j}$ (where $\overline{u_j}$ is the cell average of the exact solution) and is therefore a good indicator of the local error between the exact solution u and the numerical solution v in cell I_j.

Numerical evidence will be given in Example 1 in section 5.

5. Numerical tests. The purpose of this section is to verify our main result, Theorem 2.1 as well as Corollary 2.1, and to present numerical evidence suggesting that the rate of superconvergence proved in this paper is optimal. In most cases, we consider random meshes (that is, each cell boundary point is randomly and independently perturbed from a uniform mesh up to a given percentage) and use λ to denote the ratio of the length of the largest cell to that of the smallest one.

Example 1. We solve the following equation:

$$\begin{cases} u_t + u_x = 0, \\ u(x,0) = e^{\sin(x)}, \\ u(0,t) = u(2\pi,t). \end{cases} \tag{5.1}$$

The exact solution to this problem is

$$u(x,t) = e^{\sin(x-t)}.$$

We use ninth order strong-stability-preserving (SSP) Runge–Kutta discretization in time [14] and take $\Delta t = 0.05 h_{\min}$ to reduce the time error. Nonuniform meshes which are obtained by randomly and independently perturbing each node in a uniform mesh by up to 40% are used, and the example is tested with both $\mathcal{P}^1$ and $\mathcal{P}^2$ polynomials. The special error in Theorem 2.1 at different downwind-biased Radau points at $t = 1$ on random meshes of N cells is computed. In Table 5.1, we can observe $(2k+1)$th order superconvergence at the downwind point and $(k+2)$th order superconvergence at other Radau points. The initial solution is obtained by exactly the same way as

TABLE 5.1
The error e at the Radau points for (5.1) *when using* $\mathcal{P}^1$ *and* $\mathcal{P}^2$ *polynomials.*

				1st Radau point		2nd Radau point		Downwind point	
Polynomial	N	h_{max}	λ	Error	Order	Error	Order	Error	Order
$\mathcal{P}^1$	50	0.202	6.056	1.86E-04	-			1.34E-04	-
	100	0.111	6.169	3.76E-05	2.64			2.87E-05	2.55
	200	5.408e-02	7.339	3.89E-06	3.17			2.92E-06	3.19
	400	2.781e-02	6.956	4.90E-07	3.12			3.80E-07	3.07
$\mathcal{P}^2$	50	0.202	6.056	1.11E-06	-	1.09E-06	-	2.13E-07	-
	100	0.111	6.169	1.70E-07	3.09	1.42E-07	3.37	1.78E-08	4.10
	200	5.408e-02	7.339	1.03E-08	3.93	7.94E-09	4.04	4.28E-10	5.21
	400	2.781e-02	6.956	7.74E-10	3.89	5.81E-10	3.93	1.37E-11	5.18

mentioned in section 4.1. The downwind-biased Radau points on the interval $[-1, 1]$ are $-\frac{1}{3}$ and 1 for $\mathcal{P}^1$ polynomials, and are $\frac{-1-\sqrt{6}}{5}$, $\frac{-1+\sqrt{6}}{5}$, and 1 for $\mathcal{P}^2$ ones.

Table 5.2 shows the rate of convergence of the error ξ. We observe that the order is $k+2$, indicating that the estimate in (2.8) is sharp.

Moreover, we also test the superconvergence for the cell average. Table 5.3 shows the result for example 1 by using the method mentioned in section 4.1 as well as with L^2 and $\mathbb{P}_-$ projection for the initial discretization. From Table 5.3, we find that the convergent rates are of order $2k+1$, $k+\frac{3}{2}$, and at least $k+2$, respectively, for the three different ways of numerical initial discretization.

TABLE 5.2
The error ξ for (5.1) when using $\mathcal{P}^1$ and $\mathcal{P}^2$ polynomials.

L^2 norm of ξ			$\mathcal{P}^1$ polynomial		$\mathcal{P}^2$ polynomial	
N	h_{max}	λ	L^2 error	Order	L^2 error	Order
50	0.202	6.056	4.09E-04	-	1.85E-06	-
100	0.111	6.169	8.67E-05	2.56	2.93E-07	3.05
200	5.408e-02	7.339	8.84E-06	3.19	1.70E-08	3.99
400	2.781e-02	6.956	1.11E-06	3.12	1.29E-19	3.88

TABLE 5.3
The cell average of the error e for (5.1) when using $\mathcal{P}^1$ and $\mathcal{P}^2$ polynomials.

L^2 norm of the cell average of e				$\mathcal{P}^1$ polynomial		$\mathcal{P}^2$ polynomial	
Initial discretization	N	h_{max}	λ	L^2 error	Order	L^2 error	Order
$u_{ht} = \mathbb{P}_- u_t$	50	0.202	6.056	3.84E-04	-	5.18E-07	-
$\int_\Omega (u_h - u)dx = 0$	100	0.111	6.169	8.23E-05	2.54	4.70E-08	3.96
	200	5.408e-02	7.339	8.42E-06	3.19	1.08E-09	5.29
	400	2.781e-02	6.956	1.06E-06	3.11	3.33E-11	5.23
L^2 projection	50	0.202	6.056	3.87E-04	-	5.56E-06	-
	100	0.111	6.169	1.19E-04	1.94	1.18E-06	2.56
	200	5.408e-02	7.339	1.38E-05	3.02	1.11E-07	3.31
	400	2.781e-02	6.956	2.02E-06	2.89	7.65E-09	4.02
$\mathbb{P}_-$ projection	50	0.202	6.056	3.35E-04	-	1.07E-06	-
	100	0.111	6.169	7.38E-05	2.50	9.30E-08	4.03
	200	5.408e-02	7.339	7.72E-06	3.16	3.47E-09	4.60
	400	2.781e-02	6.956	9.81E-07	3.10	1.72E-10	4.52

Now we take the steps in section 4.5, and follow the same notation defined there. θ is taken to be $\theta = 1$, i.e., we consider the extension from the downwind cell to the right. We use $\mathcal{P}^2$ polynomials on a uniform mesh with $N = 100$. Define piecewise constants $S(x)$ such that in cell I_j

$$S(x) = S_j = \frac{\widetilde{v_j} - \overline{v_j}}{\widetilde{v_j} - \overline{u_j}} - 1,$$

where $\overline{u_j}$ denotes the cell average of the exact solution u in cell I_j. We compute and observe that $\|S\|_{\infty,\Omega} = 7.90 \times 10^{-4}$, indicating that the computable quantity $\widetilde{v_j} - \overline{v_j}$ is a good estimate of the local error $\widetilde{v_j} - \overline{u_j}$. From Figure 5.1, we can see that the computable quantity $|\bar{v} - \tilde{v}|$ captures the profile of the local error $|u - v|$ (computed at the middle point in each cell) well.

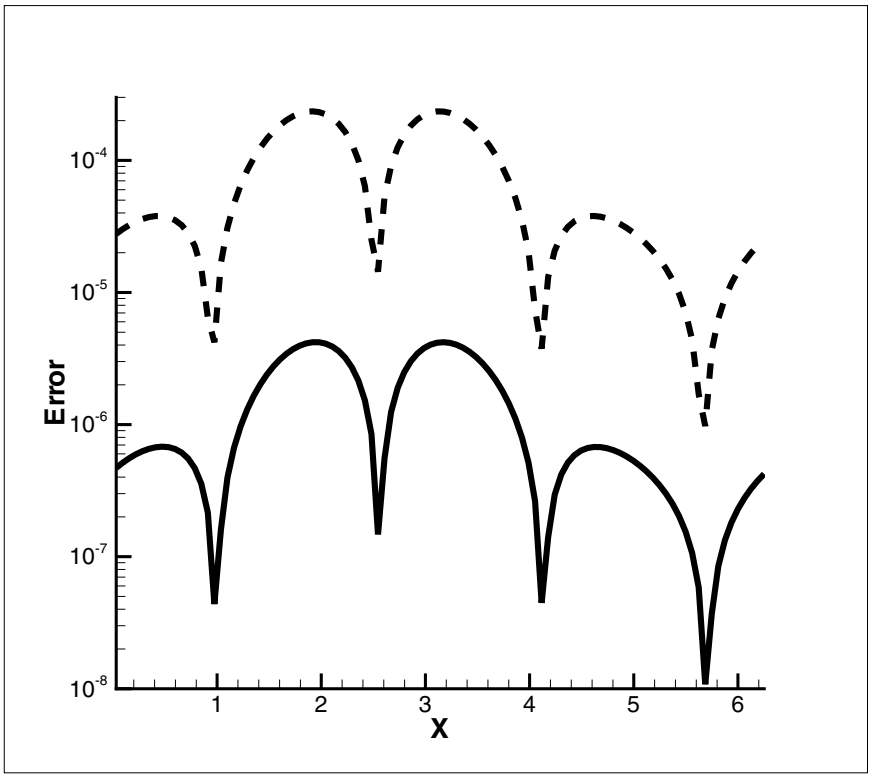

FIG. 5.1. *Comparison between $|u - v|$ (solid line) and $|\bar{v} - \tilde{v}|$ (dashed line).*

Example 2. We solve the following initial boundary value problem:

$$\begin{cases} u_t + u_x = 0, \\ u(x,0) = \sin(x), \\ u(0,t) = \sin(-t). \end{cases} \tag{5.2}$$

The exact solution to this problem is

$$u(x,t) = \sin(x - t).$$

We use third order SSP Runge–Kutta discretization in time and take $\Delta t = 0.1h_{\min}^2$ to reduce the time error, and test the example with both $\mathcal{P}^1$ and $\mathcal{P}^2$ polynomials. The same quantities as in Example 1 on the same kind of random meshes of N cells are computed. The initial solution is again obtained in the way given in section 4.1. In Table 5.4 we can observe that the error between the DG solution and the exact solution is $(2k+1)$th order superconvergent at the downwind point and $(k+2)$th order superconvergent at the other Radau points.

Table 5.5 shows the $(k+2)$th order superconvergence of the error ξ in the L^2 norm, demonstrating that the estimate in (2.8) is sharp.

As in Example 1, we also test the superconvergence for the cell average. Table 5.6 shows the result for Example 2 by using the method mentioned in section 4.1 as well as the L^2 and $\mathbb{P}_-$ projections for the initial discretization. From Table 5.6, we observe similar results as in the periodic case.

TABLE 5.4
The error e at the Radau points for (5.2) *when using* $\mathcal{P}^1$ *and* $\mathcal{P}^2$ *polynomials.*

				1st Radau point		2nd Radau point		Downwind point	
Polynomial	N	h_{max}	λ	Error	Order	Error	Order	Error	Order
$\mathcal{P}^1$	50	0.202	6.056	6.06E-05	-			2.88E-05	-
	100	0.111	6.169	8.92E-06	3.16			4.30E-06	3.14
	200	5.408e-02	7.339	1.02E-06	3.04			4.73E-07	3.09
	400	2.781e-02	6.956	1.25E-07	3.15			5.82E-08	3.15
$\mathcal{P}^2$	50	0.202	6.056	4.10E-07	-	3.11E-07	-	1.30E-08	-
	100	0.111	6.169	3.20E-08	4.21	2.38E-08	4.24	5.51E-10	5.22
	200	5.408e-02	7.339	1.84E-09	4.00	1.38E-09	3.99	1.45E-11	5.06
	400	2.781e-02	6.956	9.36E-11	4.48	1.05E-10	3.87	4.31E-13	5.28

TABLE 5.5
The error ξ *for* (5.2) *when using* $\mathcal{P}^1$ *and* $\mathcal{P}^2$ *polynomials.*

L^2 norm of ξ			$\mathcal{P}^1$ polynomial		$\mathcal{P}^2$ polynomial	
N	h_{max}	λ	L^2 error	Order	L^2 error	Order
50	0.202	6.056	1.24E-04	-	6.63E-07	-
100	0.111	6.169	1.87E-05	3.13	5.32E-08	4.17
200	5.408e-02	7.339	2.10E-06	3.06	3.03E-09	4.01
400	2.781e-02	6.956	2.58E-07	3.15	2.30E-10	3.88

TABLE 5.6
The cell average of the error e for (5.2) *when using* $\mathcal{P}^1$ *and* $\mathcal{P}^2$ *polynomials.*

L^2 norm of the cell average of e				$\mathcal{P}^1$ polynomial		$\mathcal{P}^2$ polynomial	
Initial discretization	N	h_{max}	λ	L^2 error	Order	L^2 error	Order
$u_{ht} = \mathbb{P}_- u_t$	50	0.202	6.056	1.11E-04	-	3.75E-08	-
$u_{h\,j+\frac{1}{2}}^- = \mathbb{P}_- u_{j+\frac{1}{2}}^-$	100	0.111	6.169	1.67E-05	3.12	1.63E-09	5.18
	200	5.408e-02	7.339	1.90E-06	3.04	4.07E-11	5.16
	400	2.781e-02	6.956	2.35E-07	3.14	1.14E-12	5.37
L^2 projection	50	0.202	6.056	1.86E-04	-	2.59E-06	-
	100	0.111	6.169	5.48E-05	2.02	3.59E-07	3.26
	200	5.408e-02	7.339	6.86E-06	2.91	3.11E-08	3.43
	400	2.781e-02	6.956	1.02E-06	2.87	2.86E-09	3.59
$\mathbb{P}_-$ projection	50	0.202	6.056	1.01E-04	-	2.49E-07	-
	100	0.111	6.169	1.53E-05	3.12	1.48E-08	4.66
	200	5.408e-02	7.339	1.72E-06	3.06	5.73E-10	4.55
	400	2.781e-02	6.956	2.06E-07	3.20	2.48E-11	4.72

Example 3. We solve the following two-dimensional problem:

$$\begin{cases} u_t + u_x + u_y = 0, \\ u(x, y, 0) = \sin(x + y) \end{cases} \tag{5.3}$$

with periodic boundary condition on the domain $[0, 2\pi]^2$. The exact solution is

$$u(x, y, t) = \sin(x + y - 2t).$$

We use a random rectangular mesh defined as

$$0 = x_{\frac{1}{2}} < \cdots < x_{N_x+\frac{1}{2}} = 2\pi, \quad 0 = y_{\frac{1}{2}} < \cdots < y_{N_y+\frac{1}{2}} = 2\pi,$$

TABLE 5.7
Superconvergence results for (5.3) *when using* $\mathcal{Q}^1$ *and* $\mathcal{Q}^2$ *polynomials.*

				$\mathcal{Q}^1$ polynomial		$\mathcal{Q}^2$ polynomial	
Error	$N_x \times N_y$	h_{max}	λ	L^2 error	Order	L^2 error	Order
$\|\mathbb{P}_- u - u_h\|$	10×10	0.997	3.722	2.65E-02	-	8.40E-04	-
	20×20	0.552	4.809	4.41E-03	3.04	6.97E-05	4.22
	40×40	0.270	7.339	5.12E-04	3.02	3.64E-06	4.13
	80×80	0.133	6.326	6.33E-05	2.96	2.33E-07	3.89
$\|\overline{u - u_h}\|$	10×10	0.997	3.722	4.19E-02	-	6.47E-04	-
	20×20	0.552	4.809	7.65E-03	2.88	5.26E-05	4.25
	40×40	0.270	7.339	9.12E-04	2.98	2.20E-06	4.44
	80×80	0.133	6.326	1.14E-04	2.94	1.16E-07	4.17
$\max_{i,j} \|(u - u_h)(x, y)\|$ (x,y) is the downwind-biased Radau points in $I_{i,j}$	10×10	0.997	3.722	2.28E-02	-	1.56E-03	-
	20×20	0.552	4.809	5.65E-03	2.37	1.35E-04	4.14
	40×40	0.270	7.339	6.39E-04	3.05	8.88E-06	3.81
	80×80	0.133	6.326	1.01E-04	2.62	7.15E-07	3.57
$\max_{i,j} \|(u - u_h)(x, y)\|$ (x,y) is the downwind point in $I_{i,j}$	10×10	0.997	3.722	1.99E-02	-	3.72E-04	-
	20×20	0.552	4.809	2.79E-03	3.33	4.09E-05	3.74
	40×40	0.270	7.339	3.93E-04	2.74	1.49E-07	4.64
	80×80	0.133	6.326	4.65E-05	3.02	1.34E-07	3.42

and

$$I_{i,j} = [x_{i-\frac{1}{2}}, x_{i+\frac{1}{2}}] \times [y_{j-\frac{1}{2}}, y_{j+\frac{1}{2}}].$$

We define the approximation space as

$$V_h^k = \left\{ u_h : u_h|_{I_{i,j}} \in \mathcal{Q}^k(I_{i,j}),\ 1 \le i \le N_x, 1 \le j \le N_y \right\},$$

where $\mathcal{Q}^k(I_{i,j})$ denotes all the tensor product polynomials of degree at most k in x and in y on $I_{i,j}$. The Gauss–Radau projection $\mathbb{P}_-$ is defined as follows:

$$\int_{I_{i,j}} (\mathbb{P}_- u - u) v_h dx dy = 0$$

for any $v_h \in V_h^{k-1}$,

$$\int_{y_{j-\frac{1}{2}}}^{y_{j+\frac{1}{2}}} (\mathbb{P}_- u(x_{i+\frac{1}{2}}, y) - u(x_{i+\frac{1}{2}}, y)) w_h(y) dy = 0$$

for any $w_h \in \mathcal{P}^{k-1}$,

$$\int_{x_{i-\frac{1}{2}}}^{x_{i+\frac{1}{2}}} (\mathbb{P}_- u(x, y_{j+\frac{1}{2}}) - u(x, y_{j+\frac{1}{2}})) z_h(x) dx = 0$$

for any $z_h \in \mathcal{P}^{k-1}$, and

$$\mathbb{P}_- u(x_{i+\frac{1}{2}}, y_{j+\frac{1}{2}}) = u(x_{i+\frac{1}{2}}, y_{j+\frac{1}{2}}).$$

We also use upwind flux and ninth order SSP Runge–Kutta discretization in time with $\Delta t = 0.1 h_{\min}$. We test the example with both $\mathcal{Q}^1$ and $\mathcal{Q}^2$ polynomials, and compute $\xi = u_h - \mathbb{P}_- u$, the error of the cell average, as well as the error on the downwind-biased Radau points and the downwind point. For simplicity, we do not consider the Radau points one by one, but select the one which gives the largest error in each cell. The initial solution is given by the $\mathbb{P}_-$ projection. The results are listed in Table 5.7.

It appears that similar superconvergence results are valid also in two dimensions. However, the technique of the proof in this paper, in particular the part related to the special projections, does not seem to be easily extendable to two dimensions.

6. Concluding remarks. We have studied the behavior of the error between the DG solution and the exact solution for sufficiently smooth solutions of linear conservation laws when upwind fluxes are used. We prove that under suitable initial discretization, the error between the DG solution and the exact solution is $(k+2)$th order superconvergent at the Radau points. Moreover, numerical experiments show the convergent rate is $(2k+1)$th order superconvergent at the downwind point as well as the L^2 norm of the cell average. We also prove that the DG solution is superconvergent with the rate $k+2$ towards a particular projection of the exact solution.

In future work, we will attempt to prove the superconvergent property for general initial discretization, and generalize the results to other types of PDEs and to multi-dimensions.

REFERENCES

[1] S. Adjerid and M. Baccouch, *Asymptotically exact a posteriori error estimates for a one-dimensional linear hyperbolic problem*, Appl. Numer. Math., 60 (2010), pp. 903–914.

[2] S. Adjerid, K. D. Devine, J. E. Flaherty, and L. Krivodonova, *A posteriori error estimation for discontinuous Galerkin solutions of hyperbolic problems*, Comput. Methods Appl. Mech. Engrg., 191 (2002), pp. 1097–1112.

[3] S. Adjerid and T. C. Massey, *Superconvergence of discontinuous Galerkin solutions for a nonlinear scalar hyperbolic problem*, Comput. Methods Appl. Mech. Engrg., 195 (2006), pp. 3331–3346.

[4] S. Adjerid and T. Weinhart, *Discontinuous Galerkin error estimation for linear symmetric hyperbolic systems*, Comput. Methods Appl. Mech. Engrg., 198 (2009), pp. 3113–3129.

[5] S. Adjerid and T. Weinhart, *Discontinuous Galerkin error estimation for linear symmetrizable hyperbolic systems*, Math. Comp., 80 (2011), pp. 1335–1367.

[6] P. G. Ciarlet, *Finite Element Method for Elliptic Problems*, North-Holland, Amsterdam, 1978.

[7] Y. Cheng and C.-W. Shu, *Superconvergence and time evolution of discontinuous Galerkin finite element solutions*, J. Comput. Phys., 227 (2008), pp. 9612–9627.

[8] Y. Cheng and C.-W. Shu, *Superconvergence of discontinuous Galerkin and local discontinuous Galerkin schemes for linear hyperbolic and convection-diffusion equations in one space dimension*, SIAM J. Numer. Anal., 47 (2010), pp. 4044–4072.

[9] B. Cockburn, S. Hou, and C.-W. Shu, *The Runge-Kutta local projection discontinuous Galerkin finite element method for conservation laws,* IV: *The multidimensional case*, Math. Comp., 54 (1990), pp. 545–581.

[10] B. Cockburn, S.-Y. Lin, and C.-W. Shu, *TVB Runge-Kutta local projection discontinuous Galerkin finite element method for conservation laws,* III: *One-dimensional systems*, J. Comput. Phys., 84 (1989), pp. 90–113.

[11] B. Cockburn, M. Luskin, C.-W. Shu, and E. Süli, *Enhanced accuracy by post-processing for finite element methods for hyperbolic equations*, Math. Comput., 72 (2003), pp. 577–606.

[12] B. Cockburn and C.-W. Shu, *TVB Runge-Kutta local projection discontinuous Galerkin finite element method for conservation laws,* II: *General framework*, Math. Comput., 52 (1989), pp. 411–435.

[13] B. Cockburn and C.-W. Shu, *The Runge-Kutta discontinuous Galerkin method for conservation laws,* V: *Multidimensional system*, J. Comput. Phys., 35 (1998), pp. 199–224.

[14] S. Gottlieb, C.-W. Shu, and E. Tadmor, *Strong stability-preserving high-order time discretization methods*, SIAM Rev., 43 (2001), pp. 89–112.

[15] C. Johnson and J. Pitkäranta, *An analysis of the discontinuous Galerkin method for a scalar hyperbolic equation*, Math. Comp., 46 (1986), pp. 1–26.

[16] L. Krivodonova, J. Xin, J.-F. Remacle, N. Chevaugeon, and J. E. Flaherty, *Shock detection and limiting with discontinuous Galerkin methods for hyperbolic conservation laws*, Appl. Numer. Math., 48 (2004), pp. 323–338.

[17] W. H. Reed and T. R. Hill, *Triangular Mesh for the Neutron Transport Equation*, Los Alamos Scientific Laboratory Report LA-UR-73-479, Los Alamos, NM, 1973.

[18] M. Zhang and C.-W. Shu, *An analysis of and a comparison between the discontinuous Galerkin and the spectral finite volume methods*, Comput. Fluids, 34 (2005), pp. 581–592.

[19] Q. Zhang and C.-W. Shu, *Error estimates to smooth solutions of Runge–Kutta discontinuous Galerkin methods for scalar conservation laws*, SIAM J. Numer. Anal., 42 (2004), pp. 641–666.

[20] X. Zhong and C.-W. Shu, *Numerical resolution of discontinuous Galerkin methods for time dependent wave equations*, Comput. Methods Appl. Mech. Engrg., 200 (2011), pp. 2814–2827.